SCIENCE CHINA
Information Sciences

• Supplementary File •

Extracting hidden messages of MLSB steganography based on optimal stego subset

ChunFang YANG[1, 2], XiangYang LUO[1, 2*], JiCang LU[1, 2*] & FenLin LIU[1, 2]

[1]*Zhengzhou Information Science and Technology Institute, Zhengzhou* 450001*, China;*
[2]*State Key Laboratory of Mathematical Engineering and Advanced Computing, Zhengzhou* 450001*, China*

Appendix A Proof of Lemma 1

Proof. The definition of the weighted stego pixel $s_i^{(q)}$ indicates that

$$E\left\{\left(s_i^{(q)}-x_i\right)^2\right\}=E\left\{\left(s_i-x_i+\left(2^l-1-2(s_i \bmod 2^l)\right)\frac{q}{2}\right)^2\right\}. \tag{A1}$$

Because MLSB steganography only changes the l least significant bit planes of the image, the high $(b-l)$ bits of pixels s_i and x_i must be equal. Thus, letting π_i and τ_i be the values of the l least significant bits of s_i and x_i, respectively, and substituting them into (A1) yields:

$$\begin{aligned}E\left\{\left(s_i^{(q)}-x_i\right)^2\right\}=&(1+q^2-2q)E\left\{\pi_i^2\right\}-2(1-q)E\left\{\pi_i\right\}E\left\{\tau_i\right\}+E\left\{\tau_i^2\right\}\\&+(1-q)q(2^l-1)E\left\{\pi_i\right\}-q(2^l-1)E\left\{\tau_i\right\}+\frac{q^2}{4}(2^l-1)^2.\end{aligned} \tag{A2}$$

1) If pixel s_i is a stego pixel in the stego image S, because the probabilities that the l least significant bits of the original image pixel take the values 0, 1, …, 2^l-2, and 2^l-1 are almost equivalent [1], and the embedded messages are pseudorandom bits, the expectations of π_i, τ_i, π_i^2, and τ_i^2 should be as follows:

$$E\left\{\pi_i\right\}=E\left\{\tau_i\right\}=\frac{1}{2^l}\sum_{\pi_i=0}^{2^l-1}\pi_i=\frac{2^l-1}{2}, \tag{A3}$$

$$E\left\{\pi_i^2\right\}=E\left\{\tau_i^2\right\}=\frac{1}{6}(2^l-1)(2^{l+1}-1). \tag{A4}$$

Applying (A3) and (A4) into formula (A2), one can obtain:

$$E\left\{\left(s_i^{(q)}-x_i\right)^2\right\}=\frac{(2^{2l}-1)}{12}(q-1)^2+\frac{(2^{2l}-1)}{12}. \tag{A5}$$

Because $0\leqslant q\leqslant 1$, when pixel s_i is a stego pixel in the stego image S, it follows that:

$$E\left\{\left(s_i^{(1)}-x_i\right)^2\right\}\leqslant E\left\{\left(s_i^{(q)}-x_i\right)^2\right\}\leqslant E\left\{\left(s_i^{(0)}-x_i\right)^2\right\}. \tag{A6}$$

It can be seen from the definition of the weighted stego pixel that the weighted stego pixel $s_i^{(0)}$ with weight 0 is actually equal to the pixel s_i itself; that is, $s_i^{(0)}=s_i$. Applying $s_i^{(0)}=s_i$ to (A6), the inequality (2) could be obtained. Moreover, if and only if $q=1$, the equal sign on the left side of (2) holds, if and only if $q=0$, the equal sign on the right side of (2) holds.

2) If pixel s_i is a nonstego pixel in the stego image S, the l least significant bits of s_i and x_i must be equivalent, viz. $\pi_i=\tau_i$. Therefore, formula (A2) can be transformed as follows:

$$E\left\{\left(s_i^{(q)}-x_i\right)^2\right\}=E\left\{\frac{(2^l-1-2\tau_i)^2q^2}{4}\right\}=\frac{q^2}{4}(2^l-1)^2-q^2(2^l-1)E\left\{\tau_i\right\}+q^2E\left\{\tau_i^2\right\}. \tag{A7}$$

* Corresponding author (email: xiangyangluo@126.com, lujicang@sina.com)

Applying (A3) and (A4) to (A7), one can obtain:

$$E\left\{\left(s_i^{(q)}-x_i\right)^2\right\}=\frac{(2^{2l}-1)}{12}q^2. \tag{A8}$$

Because $0\leqslant q\leqslant 1$, (A8) indicates that if pixel s_i is a nonstego pixel in the stego image S, then the inequality (3) could be obtained:

$$E\left\{\left(s_i^{(1)}-x_i\right)^2\right\}\geqslant E\left\{\left(s_i^{(q)}-x_i\right)^2\right\}\geqslant E\left\{\left(s_i^{(0)}-x_i\right)^2\right\}=E\left\{(s_i-x_i)^2\right\}=0. \tag{A9}$$

The equal sign on the left side of (3) holds if and only if $q=1$, and the equal sign on the right side of (3) holds if and only if $q=0$.

In summary, this lemma holds for MLSB steganography.

For example, when 8 bits are used to store the value of each pixel, if pixel s_i whose 2LSB is equal to 3 has been embedded message bits into by 2LSB steganography, from the definition of the weighted stego pixel, it can be obtained that $s_i^{(q)}=3-3q/2$. Because the value of the corresponding cover pixel x_i may be 0, 1, 2, or 3 with the same probability 1/4, the expectation of $\left(s_i^{(q)}-x_i\right)^2$ can be derived as follows:

$$E\left\{\left(s_i^{(q)}-x_i\right)^2\right\}=\frac{(3-3q/2)^2+(2-3q/2)^2+(1-3q/2)^2+(0-3q/2)^2}{4}=\frac{(14-18q+9q^2)}{4}. \tag{A10}$$

Similarly, it can be derived that if the 2LSB of pixel s_i is equal to 2, 1 or 0, the expectation of $\left(s_i^{(q)}-x_i\right)^2$ should respectively be

$$E\left\{\left(s_i^{(q)}-x_i\right)^2\right\}=\frac{(2-q/2)^2+(1-q/2)^2+(0-q/2)^2+(-1-q/2)^2}{4}=\frac{6-2q+q^2}{4}, \tag{A11}$$

$$E\left\{\left(s_i^{(q)}-x_i\right)^2\right\}=\frac{(1+q/2)^2+(0+q/2)^2+(-1+q/2)^2+(-2+q/2)^2}{4}=\frac{6-2q+q^2}{4}, \tag{A12}$$

or

$$E\left\{\left(s_i^{(q)}-x_i\right)^2\right\}=\frac{(0+3q/2)^2+(-1+3q/2)^2+(-2+3q/2)^2+(-3+3q/2)^2}{4}=\frac{14-18q+9q^2}{4}. \tag{A13}$$

When the embedded message bits are pseudorandom, the 2LSB of a stego pixel would take the value 3, 2, 1 and 0 with the same probability. Therefore, one can obtain the expectation of $\left(s_i^{(q)}-x_i\right)^2$ for the stego pixel as follows:

$$E\left\{\left(s_i^{(q)}-x_i\right)^2\right\}=\frac{5}{4}(q-1)^2+\frac{5}{4}. \tag{A14}$$

It can be seen that Eqn. (A14) is an example of (A5) with $l=2$. When $q=0$, the expectation is maximal; and when $q=1$, the expectation is minimal.

Appendix B Proof of Theorem 1

Proof. According to (A5) and (A8), one can obtain:

$$E\left\{\left(s_i^{(1)}-x_i\right)^2\right\}=\frac{2^{2l}-1}{12}, s_i\in S, \tag{B1}$$

$$E\left\{\left(s_i^{(0)}-x_i\right)^2\right\}=\begin{cases}\frac{2^{2l}-1}{6}, & s_i\in U;\\ 0, & s_i\in(S-U).\end{cases} \tag{B2}$$

From the definition of the weighted stego pixel, the following formula holds for the suspected stego pixels subset G of stego image S.

$$\begin{aligned}E\left\{\sum_{s_i\in G}\left(s_i^{(1)}-x_i\right)^2+\sum_{s_i\in S-G}(s_i-x_i)^2\right\}=&\sum_{s_i\in G\cap U}E\left\{\left(s_i^{(1)}-x_i\right)^2\right\}+\sum_{s_i\in G\cap(S-U)}E\left\{\left(s_i^{(1)}-x_i\right)^2\right\}\\&+\sum_{s_i\in(S-G)\cap U}E\left\{(s_i-x_i)^2\right\}+\sum_{s_i\in(S-G)\cap(S-U)}E\left\{(s_i-x_i)^2\right\}.\end{aligned} \tag{B3}$$

Because all pixels in U are stego pixels, and all pixels in $S-U$ are nonstego pixels, applying (B1) and (B2) to (B3) yields:

$$\begin{aligned}&E\left\{\sum_{s_i\in G}\left(s_i^{(1)}-x_i\right)^2+\sum_{s_i\in S-G}(s_i-x_i)^2\right\}\\=&\frac{(2^{2l}-1)}{12}|G\cap U|+\frac{(2^{2l}-1)}{12}|G\cap(S-U)|+\frac{(2^{2l}-1)}{6}|(S-G)\cap U|\\=&\frac{(2^{2l}-1)}{12}(|G\cap(S-U)|+|(S-G)\cap U|)+\frac{(2^{2l}-1)}{12}|U|,\end{aligned} \tag{B4}$$

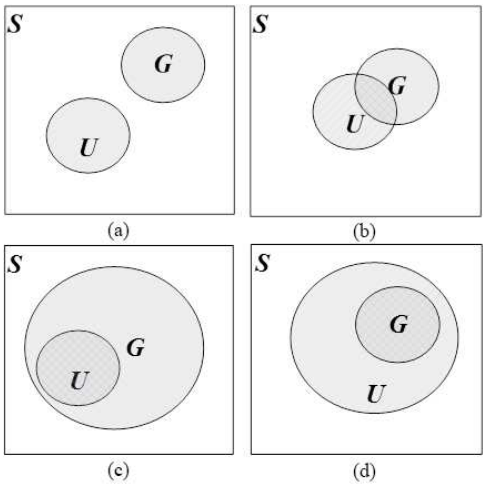

Figure B1 Four possible relationships among the stego pixel subset U and the selected pixel subset G when $U \neq G$: (a) $U \cap G = \Phi$, (b) $U \cap G \neq \phi$, $(U \cap G) \subset U$, and $(U \cap G) \subset G$, (c) $U \subset G$, (d) $G \subset U$.

where $|*|$ denotes the cardinality of set $*$.

When $G = U$, the intersection of the stego pixel subset U and the nonstego pixel set $S - U$ is empty; therefore,

$$E\left\{\sum_{s_i \in U}\left(s_i^{(1)} - x_i\right)^2 + \sum_{s_i \in S-U}(s_i - x_i)^2\right\} = \frac{2^{2l}-1}{12}|U|. \tag{B5}$$

When $G \neq U$, there are four possible cases, as shown in Figure B1. It can be seen from Figure B1 that in the cases (a) and (b), both $G \cap (S-U)$ and $(S-G) \cap U$ are not empty, viz. $G \cap (S-U) \neq \phi$ and $(S-G) \cap U \neq \phi$, and in the cases (c) and (d), one of $G \cap (S-U)$ and $(S-G) \cap U$ is not empty, viz. $G \cap (S-U) \neq \phi$ for the case of (c) and $(S-G) \cap U \neq \phi$ for the case of (d). Hence, from (B4), it can be derived that:

$$\begin{aligned} E\left\{\sum_{s_i \in U}\left(s_i^{(1)} - x_i\right)^2 + \sum_{s_i \in S-U}(s_i - x_i)^2\right\} &= \frac{(2^{2l}-1)}{12}\left(|G \cap (S-U)| + |(S-G) \cap U|\right) + \frac{(2^{2l}-1)}{12}|U| \\ &\geqslant \frac{(2^{2l}-1)}{12}|U|. \end{aligned} \tag{B6}$$

In conclusion, if and only if $G = U$ holds, the expectation $E\left\{\sum_{s_i \in G}\left(s_i^{(1)} - x_i\right)^2 + \sum_{s_i \in S-G}(s_i - x_i)^2\right\}$ can reach its minimum value $\frac{(2^{2l}-1)}{12}|U|$.

Appendix C Stego key recovering algorithm

It is assumed that the steganalyzer knows the embedding position generator that should be fed a stego key, but does not know the stego key. This case would occur under certain scenarios; for example, the steganalyzer obtains the steganography tool from the steganographer's computer, storage carrier, or communication content, or recognizes the used steganography tool based on an identification string or statistical feature. In this case, one can recover the correct stego key by Algorithm C1.

In this algorithm, the number of hidden bit planes l is determined by the steganography tool; the length of message L can be estimated by many existing effective quantitative steganalysis methods [1–4], and certain low-pass filters can be used as the estimator of the cover pixels. Therefore, it assumed that these parameters are known to the steganalyzer.

Appendix D Payload location algorithm

It is assumed that the steganalyzer does not know the embedding position generator, but possesses multiple stego images embedded in the same positions. This case would occur under certain scenarios; for example, in order to not embed too many bits into an image, the steganographer may embed message segments with the same size smaller than a given threshold into multiple images with the same size, with the same key. In this case, the steganalyzer can average $\hat{r}_{(i,j)}$ over the same position of multiple stego images to ease the impact of unchanged stego pixels, and locate the stego positions by Algorithm D1.

When the embedding positions are sequential or selected with pseudorandom intervals, one can combine the message bits in each located position to extract the secret bits. Additionally, the payload location results can be used to estimate the groups of group parity steganography [6] and determine the stego pixel order of pseudorandom steganography [7].

Algorithm C1 Stego key recovery algorithm for the case in which the steganalyzer knows the embedding position generator that should be fed a stego key, but does not know the stego key.

Require:
The given stego image, S;
the number of stego bit planes, l;
the length of message, L;
the estimator of the cover pixels.

Ensure:
The recovered stego key, $\hat{K}$.

1: Estimate the cover pixel $\hat{x}_i$ of each pixel s_i in the given stego image S using the estimator of the cover pixels;
2: According to the pixel s_i, the estimated cover pixel $\hat{x}_i$, and the parameter l, calculate the value of the corresponding term $\hat{r}_i$ using formula (6);
3: Assign a very large value to the minimum-sum variable R;
4: **for all** t such that $t \in \Omega$ **do**
5: Generate the embedding position set $\Gamma(t, L)$ containing the first L embedding positions along the embedding path;
6: Compute the sum of $\hat{r}_i$ over all positions in $\Gamma(t, L)$, and assign it to R_tmp;
7: If $R\_tmp < R$, let $\hat{K} = t$ and $R = R_{tmp}$.
8: **end for**
9: **return** the recovered stego key $\hat{K}$.

Algorithm D1 Payload location algorithm for the case in which the steganalyzer does not know the embedding position generator, but possesses multiple stego images embedded in the same positions.

Require:
The given M stego images, $S_1, S_2, \ldots, S_M$;
the number of stego bit planes, l;
the length of message, L;
the estimator of the cover pixels.

Ensure:
The estimated position set of stego pixels, $\hat{Z}$.

1: Estimate the cover pixel $\hat{x}_{i,j}$ of each pixel $s_{i,j}$ in each given stego image using the estimator of the cover pixels;
2: According to the pixel $s_{i,j}$, the estimated cover pixel $\hat{x}_{i,j}$, and the parameter l, calculate the value of the corresponding term $\hat{r}_{i,j}$ using formula (9);
3: For each position i, compute the sum of $\hat{r}_{i,j}$ over the given M stego images, and assign it to $\hat{r}_{i,*}$;
4: Select L positions with minimum $\hat{r}_{i,*}$ to construct the estimated stego position set $\hat{Z}$;
5: **return** return the estimated stego position set $\hat{Z}$.

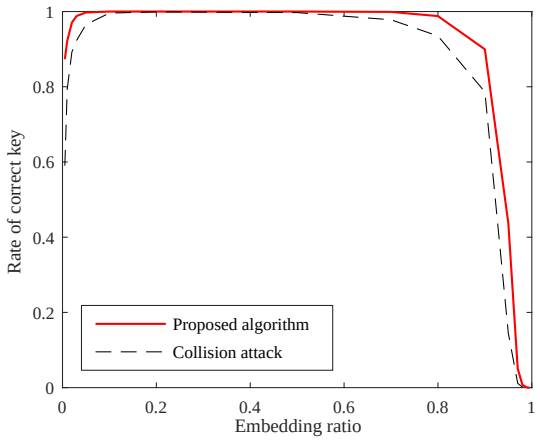

Figure E1 Rate of correct key recovery by the proposed stego key recovery algorithm and collision attack algorithm for different embedding ratios of 3LSB steganography.

Appendix E Further experimental results and analysis

Appendix E.1 Experimental setup

1) **Experimental setup for stego key recovery.** A pseudorandom embedding position generator was implemented by taking the xor of a stego key and the output of a linear feedback shifting register was fed to the stego key. Then, 32 groups of stego images with ratios 0.005, 0.01, 0.02, 0.03, 0.05, 0.10, 0.20, 0.50, 0.70, 0.80, 0.90, 0.95, 0.97, 0.98, 0.99, and 0.995 were generated by using 2LSB and 3LSB steganography to embed pseudorandom message bits into the 10000 gray cover images introduced in the main body. In each group of stego images, the stego key of each stego image was an integer randomly selected from 1 to 2^{16}. In order to evaluate the performance, the collision attack algorithm was also implemented based on the value of (6). Namely, the L positions with minimal values of (6) were regarded as the estimated modification position, and used in the collision attack. Both the collision attack algorithm and the proposed stego key recovery algorithm estimated the cover image by low-pass filtering the coefficients of 8-tap Daubechies one-level wavelet decomposition [8]. Because the variances of the stego signal in an image fully embedded by 2LSB and 3LSB steganography are 2.5 and 10.5, the noise variances in the cover image estimators for 2LSB and 3LSB steganography were set as $2.5p$ and $10.5p$, respectively. Then, the collision attack algorithm and the proposed stego key recovery algorithm were used to recover the stego key of each stego image in the 32 groups of stego images.

2) **Experimental setup for payload location.** Twenty groups of stego images were generated by embedding message into the 2LSB and 3LSB of the cover images with ratios $p = 0.05, 0.10, 0.20, \ldots, 0.90$. Images in the same group contain message in the same positions. Among the existing payload location algorithms, the wavelet absolute moments (WAM)-based algorithm is the only one that can be directly applied to locate the payload of MLSB steganography. Therefore, the proposed payload location algorithm and the WAM-based algorithm were used to locate the payload using 1, 2, ..., 10, 20, ..., 100, 200, ..., 1000, 2000, ..., 10000 stego images in each group of stego images. In order to fairly compare the performance of the two algorithms, the cover image estimator used in the proposed payload location algorithm was the same as that in the WAM-based algorithm.

Appendix E.2 Experimental results and analysis

Figure E1 shows the rate of correct stego key recovery by the proposed stego key recovery algorithm and collision attack algorithm for different embedding ratios of 3LSB steganography. From Figure 1(a) and E1, it can be seen that although both of the algorithms can correctly recover the stego key with high rates when the embedding ratio is not close to 0 or 1, the proposed algorithm outperforms the collision attack algorithm significantly. From the experiments, it is found that the rates of correct stego key recovery by the proposed algorithm are approximately 5% higher than by the collision attack algorithm when the embedding ratio of 2LSB steganography is smaller than 0.95. Even when the embedding ratio is 0.005, the correct recovery rate of the proposed algorithm is 64.47%, whereas that of the collision attack algorithm is only 21.15%.

However, when the embedding ratio of 3LSB steganography is smaller than 0.8, both the proposed Algorithm C1 and the collision attack algorithm can recover the stego key almost perfectly. This is because, when embedding message into three least significant bit planes, the stego noise should be stronger. Additionally, the sharply decreasing correct recovery rates can be seen from both ends of the lines in Figure 1(a) and E1. This should be ascribed to the decreased number of stego pixels and the decreased statistical difference between the fully embedded pixel subset and the randomly selected pixel subset, respectively.

Table E1 and E2 present the false positive rates of the proposed payload location algorithm and WAM-based algorithm for different numbers of stego images when the embedding ratios are 0.10, 0.30, 0.50, 0.70, and 0.90. It can be found that the proposed payload location algorithm outperforms the WAM-based algorithm significantly when the embedding ratio is

Table E1 False positive rate of the proposed payload location algorithm (referred to as Alg.D1) and WAM-based algorithm as a function of the number of stego images and the embedding ratio of 2LSB steganography

N	0.10		0.30		0.50		0.70		0.90	
	Alg.D1	WAM	Alg.D1	WAM	Alg.D1	WAM	Alg.D1	WAM	Alg.D1	WAM
10	80.31	39.71	**42.94**	44.05	**23.18**	37.17	**17.38**	24.45	**7.64**	9.05
20	72.97	39.01	**33.45**	35.89	**19.64**	30.33	**13.24**	20.06	**5.80**	8.10
30	70.45	24.93	**25.89**	31.33	**15.00**	25.07	**9.34**	16.12	**4.79**	7.58
40	61.97	19.87	**21.57**	28.11	**12.40**	22.07	**7.28**	15.60	**3.77**	6.86
50	61.66	17.78	**20.17**	22.87	**10.35**	18.70	**5.90**	13.84	**2.94**	6.11
60	61.44	14.77	**15.99**	21.39	**8.14**	17.49	**4.60**	13.06	**2.38**	5.85
70	51.67	11.88	**12.13**	18.74	**7.08**	15.64	**3.68**	11.61	**1.95**	5.62
80	51.46	9.80	**9.95**	17.05	**5.78**	14.56	**2.86**	10.88	**1.63**	5.36
90	46.62	9.71	**8.65**	15.25	**4.68**	13.40	**2.69**	9.95	**1.43**	4.99
100	44.87	9.48	**7.10**	14.30	**3.85**	12.49	**2.20**	9.26	**1.19**	4.58
200	29.01	6.98	**2.22**	10.32	**0.76**	7.63	**0.39**	6.19	**0.19**	2.91
500	6.62	4.55	**0.25**	4.84	**0.13**	4.38	**0.03**	2.71	**0.01**	1.42
1000	**1.78**	3.26	**0.17**	3.36	**0.10**	2.73	**0.01**	1.93	**0.00**	0.80
2000	**0.83**	2.52	**0.15**	2.67	**0.08**	1.91	**0.01**	1.32	**0.00**	0.51
5000	**0.63**	2.49	**0.14**	2.34	**0.07**	1.52	**0.01**	0.84	**0.00**	0.33
10000	**0.57**	2.41	**0.14**	2.14	**0.05**	1.34	**0.00**	0.66	**0.00**	0.29

Table E2 False positive rate of the proposed payload location algorithm and WAM-based algorithm as a function of the number of stego images and the embedding ratio of 3LSB steganography

N	0.10		0.30		0.50		0.70		0.90	
	Alg.D1	WAM	Alg.D1	WAM	Alg.D1	WAM	Alg.D1	WAM	Alg.D1	WAM
10	57.16	29.77	**25.63**	27.25	**19.95**	25.10	**15.00**	15.58	**6.26**	6.82
20	44.58	15.51	**13.20**	17.77	**10.59**	16.66	**8.21**	11.62	**4.00**	5.19
30	29.81	10.58	**7.61**	12.28	**6.12**	12.45	**5.16**	9.51	**2.89**	4.19
40	20.32	8.27	**4.71**	8.87	**3.53**	8.32	**3.70**	8.37	**1.94**	3.57
50	14.82	6.50	**2.95**	6.89	**2.23**	6.87	**2.67**	6.55	**1.33**	2.73
60	11.50	4.31	**2.04**	6.09	**1.51**	6.00	**1.79**	4.76	**0.94**	2.47
70	8.34	3.98	**1.48**	4.91	**1.06**	4.65	**1.18**	4.02	**0.67**	2.20
80	6.52	3.40	**1.01**	3.69	**0.61**	3.68	**0.77**	3.54	**0.45**	1.91
90	6.07	3.03	**0.68**	2.85	**0.38**	3.09	**0.54**	3.00	**0.32**	1.59
100	5.69	2.72	**0.50**	2.25	**0.25**	2.55	**0.41**	2.55	**0.21**	1.35
200	**0.93**	1.06	**0.05**	0.79	**0.01**	0.67	**0.03**	0.69	**0.01**	0.43
500	**0.10**	0.45	**0.01**	0.24	**0.00**	0.17	**0.00**	0.13	**0.00**	0.08
1000	**0.06**	0.33	**0.01**	0.14	**0.00**	0.10	**0.00**	0.05	**0.00**	0.03
2000	**0.06**	0.30	**0.01**	0.11	**0.00**	0.07	**0.00**	0.03	**0.00**	0.02
5000	**0.06**	0.24	**0.00**	0.08	**0.00**	0.06	**0.00**	0.02	**0.00**	0.01
10000	**0.06**	0.23	**0.00**	0.09	**0.00**	0.05	**0.00**	0.02	**0.00**	0.01

not smaller than 0.30. Even if the embedding ratio is smaller than 0.30, the proposed algorithm is still superior when one possesses enough stego images embedded in the same positions. Additionally, both of the algorithms can locate the payload of 3LSB steganography with lower false positive rates than locating the payload of 2LSB steganography. This should be ascribed to the stronger stego noise of 3LSB steganography.

References

1 Yu X Y, Tan T N, Wang Y H. Extended optimization method of LSB steganalysis. In: Proceedings of IEEE International Conference on Image Processing, Genoa, Italy, 2005. 1102-1105.

2 Yang C F, Liu F L, Luo X Y, Liu B. Steganalysis frameworks of embedding in multiple least-significant bits. IEEE Transactions on Information Forensics and Security, 2008, 3(4): 662-672.

3 Yang C F, Liu F L, Luo X Y, Zeng Y. Pixel group trace model-based quantitative steganalysis for multiple least-significant bits steganography. IEEE Transactions on Information Forensics and Security, 2013, 8(1): 216-228.
4 Yang C F, Liu F L, Lian S G, Luo X Y, Wang D S. Weighted stego image steganalysis of message hidden into each bit plane. The Computer Journal, 2012, 55(6): 717-727.
5 Goljan M, Fridrich J, Holotyak T. New blind steganalysis and its implications. In: Proceedings of SPIE 6072, Security, Steganography and Watermarking of Multimedia Contents VIII, San Jose, CA, USA, 2006. 0101-0113.
6 Quach T. Locating payload embedded by group-parity steganography. Digital Investigation, 2012, 9(2): 160-166.
7 Quach T. Extracting hidden messages in steganographic images. Digital Investigation, 2014, 11(S2): S40-S45.
8 Goljan M, Fridrich J, Holotyak T. New blind steganalysis and its implications. In: Proceedings of SPIE 6072, Security, Steganography and Watermarking of Multimedia Contents VIII, San Jose, CA, USA, 2006. 0101-0113.